
Random-Set Graph Neural Networks

Tommy Woodley
School of Engineering,
Computing and Mathematics
Oxford Brookes University
19204799@brookes.ac.uk

Shireen Kudukkil Manchingal
School of Engineering,
Computing and Mathematics
Oxford Brookes University
smanchingal@brookes.ac.uk

Matteo Tolloso
Department of Computer Science
University of Pisa
matteo.tolloso@phd.unipi.it

Davide Bacciu
Department of Computer Science
University of Pisa
davide.bacciu@unipi.it

Fabio Cuzzolin
Oxford Brookes Institute for
Artificial Intelligence,
Data Analysis and Systems (AIDAS)
fabio.cuzzolin@brookes.ac.uk

Abstract

Uncertainty quantification has become an important factor in understanding the data representations produced by Graph Neural Networks (GNNs). Despite their predictive capabilities being ever useful across industrial workspaces, the inherent uncertainty induced by the nature of the data is a huge mitigating factor to GNN performance. While aleatoric uncertainty is the result of noisy and incomplete stochastic data such as missing edges or over-smoothing, epistemic uncertainty arises from lack of knowledge about a system or model (e.g., a graph’s topology or node feature representation), which can be reduced by gathering more data and information. In this paper, we propose an original new framework in which node-level epistemic uncertainty is modelled in a belief function (finite random set) formalism. The resulting Random-Set Graph Neural Networks have a belief-function head predicting a random set over the list of classes, from which both a precise probability prediction and a measure of epistemic uncertainty can be obtained. Extensive experiments on 9 different graph learning datasets, including real-world autonomous driving benchmarks as such Nuscene and ROAD, demonstrate RS-GNN’s superior uncertainty quantification capabilities.

1 Introduction

Machine learning systems are increasingly deployed in safety-critical domains, where erroneous predictions may lead to severe consequences. In such settings, it is not sufficient for a model to be accurate; it must also be aware of its own limitations; in other words, to know when it does not know [Manchingal and Cuzzolin, 2022, Manchingal, 2025]. A central obstacle to trustworthy deployment is the reliable quantification of *epistemic uncertainty*, the uncertainty arising from limited knowledge about the data-generating process [Kendall and Gal, 2017, Hüllermeier and Waegeman, 2021].

This challenge is particularly acute for Graph Neural Networks (GNNs) [Scarselli et al., 2008]. Unlike classical learning in which data points are i.i.d. (independent and identically distribute), graph data exhibits strong relational dependencies between instances: uncertainty, therefore, can originate not

only from noisy node features but also from structural ambiguity in the graph topology [Khan et al., 2018, Wang et al., 2024a]. A node may be uncertain because its neighborhood is inherently ambiguous (aleatoric uncertainty), or because its structural context is novel and insufficiently represented in the training data (epistemic uncertainty). Topological uncertainties are a factor in signal processing [Ceci and Barbarossa, 2020], wireless networks [Coon, 2016] and multi-agent systems [Yucelen et al., 2015], to cite just a few examples. Disentangling these sources is essential for robust out-of-distribution (OOD) detection [Yang et al., 2024] and reliable graph learning [Gawlikowski et al., 2023, Valdenegro-Toro and Mori, 2022].

Bayesian approaches provide a principled lens for this decomposition by marginalizing predictions over a posterior distribution of model parameters [Malinin and Gales, 2018]. In Graph Neural Networks, Bayesian variants place distributions over weights and, in some cases, over graph structure itself [Hasanzadeh et al., 2020, Munikoti et al., 2023]. However, Bayesian Graph Neural Networks often incur substantial computational overhead and require carefully specified priors [Goan and Fookes, 2020, Wang et al., 2024b]. Ensemble-based approaches offer a practical alternative by measuring disagreement across independently trained models [Lakshminarayanan et al., 2017, Mallick et al., 2022], yet they scale poorly and remain limited to first-order probability representations. Recent work has explored *credal learning* on graphs [Tollosio and Bacciu, 2025], where models output probability intervals [De Campos et al., 1994, Pearl, 1988, Cuzzolin, 2007a, 2009, 2022] forming a credal set [Caprio et al., 2024, Wang et al., 2024c]. While credal methods provide expressive set-valued predictions and principled uncertainty decompositions, they operate within the space of probability distributions. A recent review of uncertainty quantification in neural networks can be found in [Wang et al., 2025a].

A recent wave of results in classification, uncertainty quantification and out-of-distribution detection using both *random-set* [Manchingal et al., 2023, 2025a, Manchingal, 2025, Manchingal et al., 2025b,c] and *credal set* representations [Caprio et al., 2023, Sale et al., 2023, Caprio et al., 2024, 2025, Wang et al., 2025b, 2024d,e], is providing significant evidence that second-order uncertainty theory [Cuzzolin, 2021, 2024] is a most promising framework for tackling the above challenges (as also supported by the results of the recent Epistemic AI [Cuzzolin and Sultana, 2024] Horizon 2020 project^{1,2}). Random sets [Nguyen and Wang, 1997, Ross, July 1986, Smets, 1992, Manchingal et al., 2024, Cuzzolin, 2023, Goutsias et al., December 1997, Ha et al., 2009], in particular, offer a more fundamental representation of epistemic uncertainty. A random set is a set-valued random variable that assigns probability mass directly to subsets of outcomes [Molchanov, 1997, 1999, 2005, Shafer, 1976]. On finite domains, random sets take the form of *belief functions* [Cuzzolin, 2014, September 2014, 2018a, 2020], which generalize classical probability measures and naturally induce a convex set of consistent probability distributions (a credal set) [Levi, 1980, Cuzzolin, 2018b].

In the recently proposed Random-Set Neural Networks (RS-NN) Manchingal et al. [2025a], predictions are expressed as belief functions over the class list, encoding epistemic uncertainty through the size and geometry of the associated credal set. A point prediction can then be recovered via the pignistic transformation [Smets and Kennes, 1994], corresponding geometrically to the center of mass of the credal set. The approach has recently been extended to large language models [Mubashar et al., 2025], generative adversarial networks [Mubashar and Cuzzolin, 2026] and Dirichlet random-set representations in a network’s parameter space [Sultana et al., 2025].

While RS-NNs have demonstrated strong performance in image classification and OOD detection, their formulation assumes independent data. Extending random-set learning to graphs, therefore, introduces new conceptual and technical challenges. Message passing in GNNs violates the i.i.d. assumption by construction, and information about a node’s label is progressively gained and lost across layers [Fuchsgruber et al., 2025]. In heterophilic graphs, where connected nodes may belong to different classes, smoothing mechanisms can blur class boundaries and exacerbate epistemic uncertainty [Zhu et al., 2020, Lim et al., 2021]. A random-set formulation must therefore account for the distinctive dynamics of graph information propagation. While message passing in the form of belief functions has been studied in the early Nineties, mostly by Shenoy and Shafer [Shenoy and Shafer, 1990, 1986, Shenoy, 2023], the problem has been never tackled from a machine learning perspective.

¹<https://www.epistemic-ai.eu/>

²<https://cordis.europa.eu/project/id/964505/results>

In this paper, we introduce *Random-Set Graph Neural Networks (RS-GNNs)*, the first framework to extend random-set neural learning to the graph domain. RS-GNN replaces the classical softmax layer of a GNN with a belief-output layer that predicts mass functions over a budgeted collection of focal sets. Each node is thus mapped to a belief function, which is mathematically equivalent to a credal set of probability distributions on the class list. The pignistic probability provides a central prediction, while the geometry of the induced credal set quantifies epistemic uncertainty.

Our approach inherits the theoretical advantages of random sets, namely, the ability to model second-order uncertainty without committing to a precise probability distribution, while adapting them to graph-structured data. By integrating belief-function outputs with message-passing representations, RS-GNN provides a principled and scalable framework for epistemic uncertainty quantification in node classification and OOD detection.

Main Contributions. Our contributions are threefold: (i) we introduce Random-Set Graph Neural Networks (RS-GNNs), extending belief-function learning to graph-structured data; (ii) we develop a budgeted focal-set selection strategy compatible with graph representations, ensuring scalability to large class spaces; and (iii) we demonstrate through extensive experiments on a large variety of homophilic and heterophilic benchmarks (including the major real-world autonomous driving datasets nuscenec [Caesar et al., 2020] and ROAD [Singh et al., 2022]) that RS-GNN achieves competitive classification performance while providing more reliable epistemic uncertainty estimates and improved OOD detection.

2 Related Work

Quantifying uncertainty in Graph Neural Networks (GNNs) [Bacciu et al., 2020] has emerged as an important and fast-evolving research area, with numerous recent methods aimed at assessing the reliability of GNN predictions [Wang et al., 2024b, Chen et al., 2024]. The intrinsic interdependencies among graph nodes pose distinctive challenges, giving rise to a wide range of uncertainty estimation strategies. Existing methods can generally be categorized into three principal families, each characterized by different computational and modeling properties.

The most computationally efficient category is that of *Single Deterministic Models*. The most basic techniques in this group rely on post-hoc heuristics applied to the outputs of a standard GNN, such as adopting the maximum softmax probability as a confidence score or computing predictive entropy. Although straightforward to implement, these methods yield a single, undifferentiated notion of uncertainty and are often susceptible to model miscalibration [Guo et al., 2017]. A more principled deterministic alternative is evidential deep learning, in which the GNN is trained to predict the parameters of a higher-order Dirichlet distribution. This formulation enables direct modeling of uncertainty over the categorical output space within a single forward pass, offering a more expressive representation of predictive uncertainty [Zhao et al., 2020, Stadler et al., 2021a]. Energy-based approaches have also recently been introduced as a deterministic framework [Wu et al., 2023]. Wang et al. [2021] introduced a post-hoc calibration mapping that adjusts the logits of a GNN while preserving their relative ordering across classes. More recently, the Graph Energy-Based Model (GEBM) [Fuchsgruber et al., 2024] derives epistemic uncertainty in a post-hoc manner from the logit-based energy of a pre-trained GNN. This approach regularizes the joint energy to ensure an integrable density and aggregates energy across multiple structural scales, all while retaining strong computational efficiency. In contrast to Bayesian or ensemble-based methods, it does not require retraining and can be readily applied to any logit-based GNN architecture.

A second prominent paradigm is *Bayesian Graph Neural Networks (Bayesian GNNs)*, which extend the Bayesian framework to graph-structured data. In these models, priors are defined not only over conventional network parameters (e.g., weights) but also over graph-specific elements such as edge connectivity and node feature propagation. For instance, adaptive connection sampling [Hasanzadeh et al., 2020] models edges (or adjacency masks) as random variables, while inference techniques such as Monte Carlo Dropout [Gal and Ghahramani, 2016] or Variational Inference [Hoffman et al., 2013] are employed to approximate posterior distributions by sampling both model parameters and possible graph realizations at prediction time. This captures uncertainty arising both from the model parameters and from the implications of the graph structure and features. Recent work, such as Munikoti et al. [2023], highlights how Bayesian approaches on graphs account for uncertainty not only in weights but also in graph topology, node attributes, and edge sampling. Along similar

lines, Stadler et al. [2021b] introduced the Graph Posterior Network (GPN), which performs explicit Bayesian posterior updates for predictions over interdependent nodes. While these methods offer a principled framework for modeling uncertainty originating from both model parameters and graph data (structure and features), they typically incur increased computational cost [Jia et al., 2020] and require careful design of appropriate priors over graph components.

Bridging the divide between theoretical soundness and practical scalability, *Ensemble Methods* have emerged as a widely adopted and effective alternative. This paradigm combines the predictions of multiple independently trained GNNs, with uncertainty quantified through the level of disagreement or variance across individual model outputs [Mallick et al., 2022, Busk et al., 2023]. Although empirically strong—and often competitive with or superior to more sophisticated Bayesian approaches—ensembles impose considerable computational and memory overhead, as they necessitate training and maintaining multiple complete models.

3 Methodology

3.1 Approach: Node-level representation

We now introduce Random-Set Graph Neural Networks (RS-GNN), a belief-function-based extension of Graph Neural Networks (Fig. 1) for epistemic uncertainty quantification on graph-structured data. RS-GNN performs belief-function encoding at the *node level* (Fig. 2): each node v is assigned a belief function defined over a shared focal-set budget \mathcal{F} . This design follows directly from the node-classification objective, where the relevant uncertainty concerns the class membership of individual nodes given their features and structural context. *Node-level* belief assignments provide localized epistemic uncertainty estimates tied to each node’s neighborhood, enabling fine-grained OOD detection and calibrated decision-making.

Encoding belief at the whole-graph level would instead capture global model-level uncertainty, which is appropriate for graph-classification tasks but unsuitable for node-level OOD detection. Conversely, encoding beliefs at the edge level would unnecessarily complicate training and interpretation without improving node classification performance. Therefore, assigning belief functions per node provides the most natural and scalable formulation for RS-GNN. In Fig. 2, intermediate representations are annotated as Z^{Bel} , Z^{Mass} , and Z^{BetP} to visually distinguish belief features, mass logits, and pignistic probabilities.

3.2 Belief function head

Let $\mathcal{Y} = \{1, \dots, C\}$ denote the set of node classes and $2^{\mathcal{Y}}$ its power set. In belief-function theory [Shafer, 1976, Cuzzolin, September 2014], uncertainty is represented by assigning *belief values* $\text{Bel}(A)$ to subsets $A \subseteq \mathcal{Y}$. Such belief values can be interpreted as lower bounds to the (epistemically uncertain) probability of A , while the dual *plausibility values* $\text{Pl}(A) = 1 - \text{Bel}(A^c)$ amount to upper bounds:

$$\text{Bel}(A) \leq P(A) \leq \text{Pl}(A). \tag{1}$$

For a good introduction to belief functions and lower probabilities, please refer to [Cuzzolin, 2024].

In principle, a belief function is defined over the entire power set $2^{\mathcal{Y}}$, containing an exponential number (2^C) of subsets. To ensure scalability, RS-GNN operates on a *budgeted focal set* $\mathcal{F} \subseteq 2^{\mathcal{Y}}$ that includes all singleton classes and a selected number of non-singleton subsets. By default, focal sets are generated as all non-empty subsets of the ID class set (full power set). For larger class spaces, the code includes an optional budgeted alternative based on a TSNE+GMM overlap as in RS-NN [Manchingal et al., 2025a].

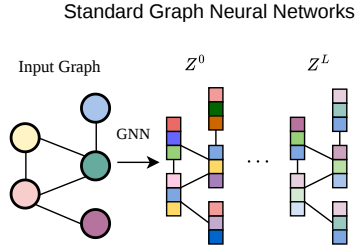


Figure 1: Standard GNN pipeline for node classification, where message passing produces node embeddings followed by a softmax probability vector.

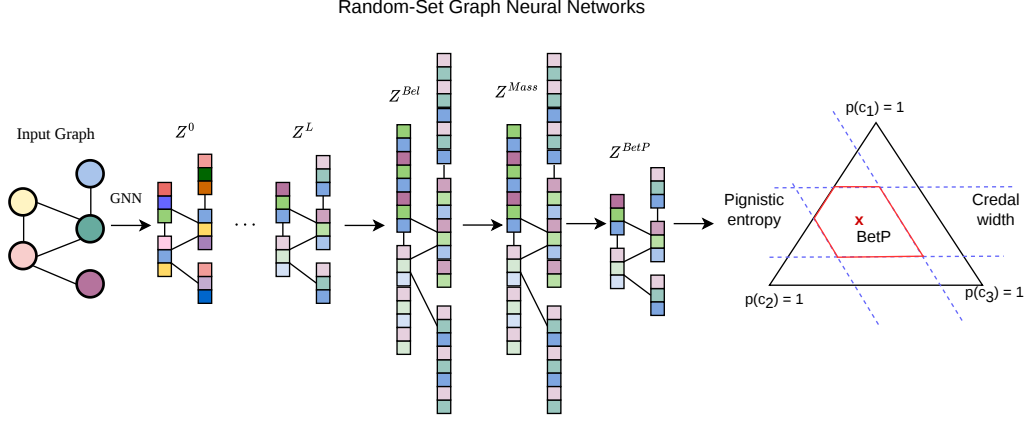


Figure 2: **Overview of the Random-Set Graph Neural Network (RS-GNN).** RS-GNN replaces the softmax layer with a belief head that outputs a mass function m_v over a budgeted collection of focal sets \mathcal{F} (singletons plus selected subsets). From the predicted mass function we derive (i) a pignistic probability vector BetP_v for point prediction and (ii) singleton lower and upper probabilities defining the induced credal set. On the right is its geometric interpretation in the 3-class probability simplex. The red polygon represents the credal set induced by m_v ; its center corresponds to the pignistic probability (red cross), whose entropy defines the pignistic entropy. The vertical span of the credal set along the predicted class axis corresponds to the credal set width used as an epistemic uncertainty score.

In our proposed framework, the RS-GNN backbone computes node representations

$$Z^l = \Phi^l(Z^{l-1}, \Psi(Z^{l-1})), \quad (2)$$

and the final-layer embedding Z_v^L is fed into a belief head that directly predicts belief values

$$\hat{\text{Bel}}_v(A_k) \in (0, 1), \quad A_k \in \mathcal{F}. \quad (3)$$

Given predicted beliefs, *mass values* $m(A)$ (i.e., probabilities that the correct output is *exactly* the set A) can be obtained using the Möbius inverse formula [Grabisch, 2004, Cuzzolin, 2008a, 2010a]

$$\hat{m}_v(A) = \sum_{B \subseteq A} (-1)^{|A \setminus B|} \hat{\text{Bel}}_v(B), \quad A \in \mathcal{F}. \quad (4)$$

To amount to a proper belief function, the mass function so obtained must satisfy non-negativity and normalisation constraints [Shafer, 1976], which are enforced through regularisation. The *pignistic probability* [Smets, 2002, 2005] (the center of mass of the credal set (1) corresponding to a belief function [Cuzzolin, 2008b, 2010b]) can then be computed from the derived mass function as follows:

$$\text{BetP}_v(i) = \sum_{A_k \ni i} \frac{\hat{m}_v(A_k)}{|A_k|}. \quad (5)$$

The pignistic probability [Smets et al., 1989, Sudano, 2015] has the meaning of a central estimate of what the correct categorical probability distribution over the classes is, given the epistemic uncertainty represented by the predicted belief function³.

The predicted class is $\hat{y}_v = \arg \max_i \text{BetP}_v(i)$.

3.3 Uncertainty quantification

In our RS-GNN framework, uncertainty is quantified using two measures. The **pignistic entropy**

$$H_v = - \sum_{i=1}^C \text{BetP}_v(i) \log(\text{BetP}_v(i) + \varepsilon), \quad (6)$$

³Note that other *probability transforms* are possible, e.g., the orthogonal projection [Cuzzolin, 2007b], the intersection probability [Cuzzolin, 2007c] as well as the relative belief [Cuzzolin, 2008c, 2012] and plausibility [Cobb and Shenoy, 2006, Cuzzolin, 2010c] of singletons.

i.e., the Shannon entropy of the predicted pignistic probability, captures predictive uncertainty. Epistemic uncertainty, instead, is measured via **credal set width** [Sale et al., 2023]. For singleton sets (individual classes), in particular,

$$\underline{P}_v(i) = \hat{m}_v(\{i\}), \quad \overline{P}_v(i) = \sum_{A_k: i \in A_k} \hat{m}_v(A_k), \quad (7)$$

and the epistemic uncertainty is the width of the corresponding probability interval (upper bound minus lower bound):

$$W_v = \overline{P}_v(\hat{y}_v) - \underline{P}_v(\hat{y}_v). \quad (8)$$

3.4 Loss function and training

Training is performed directly in belief space. For a node with ground-truth label y_v , the target belief encoding is

$$\text{Bel}_v^{\text{target}}(A) = \mathbf{1}\{y_v \in A\}. \quad (9)$$

The latter encodes the fact that all sets of classes containing y_v are possible correct predictions, under random-set epistemic uncertainty, so the belief function should assign to them a belief of 1.

The primary loss is binary cross-entropy over focal sets:

$$\mathcal{L}_{\text{Bel}} = - \sum_v \sum_{A_k \in \mathcal{F}} \left[\text{Bel}_v^{\text{target}}(A_k) \log(\hat{\text{Bel}}_v(A_k)) + (1 - \text{Bel}_v^{\text{target}}(A_k)) \log(1 - \hat{\text{Bel}}_v(A_k)) \right]. \quad (10)$$

To ensure that the derived mass function is valid, we include regularisation terms that penalise negative mass values and deviations from normalisation:

$$\mathcal{R}(m) = \alpha \sum_{A_k \in \mathcal{F}} \max(0, -\hat{m}_v(A_k)) + \beta \left| \sum_{A_k \in \mathcal{F}} \hat{m}_v(A_k) - 1 \right|. \quad (11)$$

The final objective function is therefore:

$$\mathcal{L} = \mathcal{L}_{\text{Bel}} + \mathcal{R}(m). \quad (12)$$

4 Experiments

4.1 Datasets

We evaluate our method on a diverse suite of nine benchmark graph datasets, encompassing various domains and structural properties.

The `Coauthors` dataset is a computer science co-authorship network where nodes represent authors, connected by an edge if they have co-authored a paper [Shchur et al., 2018]. Node features are derived from paper keywords, and the task is to predict each author’s primary field of study. The `Chameleon` and `Squirrel` datasets⁴ are Wikipedia networks where nodes are web pages linked by hyperlinks [Rozemberczki et al., 2021]. Their features are derived from informative nouns on each page, and the classification task is to categorize pages based on their average monthly traffic. `Reddit2` is a dataset constructed from Reddit posts, where nodes represent individual posts with features generated from text embeddings [Hamilton et al., 2017]. An edge connects two posts if the same user has commented on both, and the prediction task is to identify the subreddit to which each post belongs. `ArXiv` is a citation network where nodes are academic papers and directed edges represent citations [Hu et al., 2020, Ma et al., 2024]. Node features are embeddings of the paper’s title and abstract, and the objective is to predict the publication year. The `Roman Empire` dataset [Platonov et al., 2023] is based on the English Wikipedia article about the Roman Empire, selected for its length and linguistic diversity. Each node corresponds to a (non-unique) word in the text, and two nodes are connected if the corresponding words either appear consecutively in the text or are linked in the dependency tree of a sentence. Node classes correspond to syntactic roles (specifically, the 17 most frequent roles

⁴While these two datasets have been criticized for having train-test data leakage (derived by duplicate nodes) [Platonov et al., 2023], they are still widely used in the literature.

plus an additional class grouping all others). Node features are derived from word embeddings. The `Amazon-Ratings` [Platonov et al., 2023] dataset is derived from the Amazon product co-purchasing network. Nodes represent products, and edges connect products that are frequently bought together. The task is to predict the average product rating, grouped into five discrete classes. Node features are computed as the mean of word embeddings of words appearing in the product descriptions. The `Cora` dataset [Yang et al., 2016] consists of scientific publications represented as nodes, with edges indicating citation links between them. Node features correspond to bag-of-words representations of document content, and the classification task is to assign each publication to its corresponding research topic. Finally, `Patents` is a citation network of U.S. utility patents, where each node is a patent and edges indicate citations between them [Leskovec et al., 2005, Lim et al., 2021, Ma et al., 2024]. Features are derived from patent metadata, and the task is to predict the patent’s grant date.

4.2 Setting

We address the problem of node-level out-of-distribution (OOD) detection in a transductive setting using a *Leave-Out-Class* strategy during training.

Let $G = (\mathcal{V}, \mathcal{E}, X)$ denote a single attributed graph, where \mathcal{V} is the set of nodes, \mathcal{E} is the set of edges, and $X \in \mathbb{R}^{|\mathcal{V}| \times d}$ is the node feature matrix. The set of all node classes is partitioned into in-distribution (ID) classes \mathcal{C}_{ID} and out-of-distribution (OOD) classes \mathcal{C}_{OOD} , such that $\mathcal{C}_{ID} \cap \mathcal{C}_{OOD} = \emptyset$.

The node set \mathcal{V} is divided into training, validation, and test subsets. During training, nodes belonging to OOD classes in \mathcal{C}_{OOD} are masked, i.e., their labels are treated as unknown. Consequently, the model is trained to solve a classification problem over only the ID classes \mathcal{C}_{ID} . Importantly, in this setting, the true labels of test nodes may include both ID and OOD classes, i.e., the test classes form a superset of the training classes.

The objective is to learn a model able to classify the in-distribution nodes into their respective classes within \mathcal{C}_{ID} and produce a high uncertainty score for nodes belonging to the OOD classes.

4.3 Baselines

We evaluate our proposed credal learning approaches against a suite of established baselines for uncertainty estimation and OOD detection [Ma et al., 2024]. These include a family of widely-used post-hoc methods that operate on a single pre-trained GNN, such as the `Energy-based score`, which is calculated from the pre-softmax logits [Liu et al., 2020]; `ODIN`, which applies temperature scaling and input perturbations [Liang et al., 2017], `CaGCN` [Wang et al., 2021], a post-hoc calibration method for logits, and the `Mahalanobis` baseline, which measures the distance of a test sample’s latent representation from the training data’s class-conditional distributions [Lee et al., 2018]. Similarly, we employ a `K-Nearest Neighbors (KNN)` approach, where uncertainty is derived from the average latent-space distance to the nearest training samples [Sun et al., 2022]. We also compare against a method specifically designed for graph data, namely `GNNSafe` [Wu et al., 2023] and the recent `GEBM` [Fuchsgruber et al., 2024].

However, the de-facto reference model against which new uncertainty quantification methods are measured is the `Classical Ensemble`. Despite its conceptual simplicity, this approach consistently achieves state-of-the-art performance across a wide range of tasks and datasets, making it the target method to outperform [Lakshminarayanan et al., 2017, Ovadia et al., 2019, Gustafsson et al., 2020, Abe et al., 2022]. Its strength lies in its combination of high performance with practical simplicity: it is easy to implement, scales effectively, and is largely hyperparameter-free, requiring only the independent training of multiple standard models.

4.4 Random-Set Graphs for Road Scene Understanding

We now evaluate Random-Set Graph Neural Networks (RS-GNNs) for road scene understanding in our temporal scene-graph pipeline. In this report, *road scene understanding* is treated as **risk-aware structured perception**: given a short temporal window, the model must (i) infer semantic categories for traffic entities (node-level recognition) and (ii) quantify uncertainty so that downstream modules (e.g., tracking, behavior prediction, planning) can handle ambiguous or novel situations conservatively rather than acting on overconfident errors.

Table 1: OOD detection performance across all datasets (AUROC \uparrow) for baseline methods. Best results are highlighted in **bold**, second-best are underlined, and third-best are shown with a light gray background.

Method	Chameleon	Squirrel	ArXiv	Patents	Amazon-Ratings	Roman Empire	Coauthor	Reddit2	Cora
Energy	58.25	44.47	50.16	43.33	51.42	52.26	94.47	43.93	12.59
KNN	56.81	52.79	56.86	52.55	<u>52.46</u>	29.32	88.23	65.63	84.67
ODIN	57.98	47.28	48.16	43.21	46.23	53.98	94.17	43.09	71.65
Mahalanobis	51.82	53.79	59.52	58.72	49.66	67.26	82.49	68.98	80.26
GNNSafe	50.42	35.88	35.30	27.35	49.50	50.28	<u>94.82</u>	61.99	88.85
Classical ensemble	74.00/30.22	58.32/59.13	58.20/65.45	48.23/60.35	48.51/51.36	46.49/55.39	<u>95.30/94.81</u>	58.84/ <u>72.09</u>	75.85/43.84
JLDE	70.06	71.06	45.35	46.74	51.72	31.01	32.37	36.55	55.36
GEBM	45.41	43.00	56.26	54.49	48.79	62.62	92.20	54.49	<u>87.15</u>
CaGCN	73.77	60.05	58.30	54.15	51.52	<u>68.03</u>	96.38	91.13	81.03

Table 2: OOD detection performance across all datasets (AUROC \uparrow) for credal-based methods and RS-GNN. Best results are highlighted in **bold**, second-best are underlined, and third-best are shown with a light gray background.

Method	Chameleon	Squirrel	ArXiv	Patents	Amazon-Ratings	Roman Empire	Coauthor	Reddit2	Cora
Credal final	<u>76.29</u> / 67.27	<u>75.02</u> / 65.85	64.65 / <u>65.66</u>	<u>68.92</u> / 69.73	51.89 / 48.11	31.51 / <u>68.48</u>	74.80 / 50.74	70.57 / 69.35	43.79 / 56.17
Credal ensemble	74.98 / 29.54	59.03 / 53.66	58.05 / 50.97	47.41 / 64.64	48.59 / 51.17	45.90 / 53.06	93.85 / 93.72	61.16 / 57.72	75.17 / 36.42
Credal frozen	48.97 / 85.67	73.03 / 26.96	42.36 / 70.22	33.29 / 68.97	52.41 / 48.78	68.05 / 69.75	93.38 / 43.78	64.69 / <u>73.63</u>	84.97 / 17.33
CredalLJ	<u>72.37</u> / <u>77.67</u>	73.89 / 77.04	<u>65.77</u> / 63.79	70.78 / 60.06	52.82 / 47.27	31.45 / 65.68	86.58 / 70.88	66.35 / 67.31	83.26 / 21.95
RandomSet GNN	84.18 / <u>84.10</u>	63.57 / 63.56	<u>70.21</u> / 69.39	49.32 / 42.14	51.05 / 50.81	69.58 / 69.39	85.72 / 74.56	67.38 / 66.85	88.84 / 88.51

Formally, each temporal window is represented as a graph

$$\mathcal{G} = (\mathcal{V}, \mathcal{E}, X), \quad (13)$$

where nodes \mathcal{V} represent scene context and traffic entities, edges \mathcal{E} represent spatial/temporal relations, and X are node features. Each labeled agent node v has a semantic class $y_v \in \{0, \dots, C-1\}$, and the primary task is node classification on labeled nodes:

$$\hat{y}_v = \arg \max_{i \in \{0, \dots, C-1\}} p(i | v, \mathcal{G}). \quad (14)$$

In addition, we evaluate out-of-distribution (OOD) detection under a strict leave-out-class protocol, where a subset of classes is removed from training supervision and only appears at validation/test time. In this setting, good road-scene understanding means not only high ID accuracy, but also *reliable epistemic uncertainty*: OOD nodes should be assigned high uncertainty scores, and ID nodes should not be spuriously flagged.

4.4.1 Datasets and Temporal Graph Construction

We evaluate RS-GNN in two complementary settings: (i) strict leave-out-class OOD within each dataset (ROAD and nuScenes), and (ii) cross-dataset OOD (train on ROAD ID, test OOD on nuScenes). All experiments use the same temporal node-graph pipeline. Dataset statistics are summarized in Tab. 3.

ROAD Dataset. Our ROAD benchmark Singh et al. [2022] contains urban and suburban driving scenes with strong variability in illumination, weather, and traffic density. Annotations include object-level labels and geometric context sufficient for graph construction at each frame. The benchmark is particularly suitable for uncertainty analysis because it includes rare classes and rare interaction patterns (e.g., unusual merges, occlusions at intersections, temporary road layouts), which naturally induce epistemic uncertainty. Following our leave-out-class protocol, a subset of classes is treated as ID during training, while OOD classes appear only at validation/test time. This setup directly tests whether uncertainty scores assign high epistemic uncertainty to unseen semantic patterns.

ROAD temporal node graphs. ROAD provides dense temporal annotations with 10 agent categories, 19 action attributes, and 12 location attributes. Each frame contributes one unlabeled scene node and one node per annotated agent. Intra-frame edges are scene-centered (scene node connected bidirectionally to all agents). Temporal edges connect scene-to-scene nodes across adjacent frames and same-tube_uid agent nodes across adjacent frames; self-loops are added. We use:

$$\text{window size} = 4, \quad \text{window stride} = 4, \quad \text{frame step} = 5. \quad (15)$$

Node features concatenate box geometry, action one-hot, location one-hot, and node-type indicators; agent-ID features are excluded to prevent leakage. Exported ROAD graphs use 37-dimensional

features, with 49,123 train graphs, 26,302 val graphs, and 26,301 test graphs (291,197 labeled test nodes).

nuScenes. We additionally evaluate on nuScenes [Caesar et al., 2020], a large-scale autonomous-driving benchmark with 1000 scenes and synchronized multi-modal sensing. The dataset provides: (i) 6 surround-view cameras, (ii) 1 LiDAR sensor, (iii) 5 radars, (iv) ego-pose and localization metadata, and (v) map priors for supported regions. Its geographic and temporal diversity (day/night transitions, weather variability, dense urban traffic) creates a robust testbed for OOD uncertainty behavior in graph models. We construct scene graphs from fused detections and map elements, using the same graph-building pipeline as for the Road Dataset to ensure a controlled comparison.

Table 3: Temporal-graph dataset statistics used in the reported runs.

Dataset	#Train graphs	#Val graphs	#Test graphs	#Test labeled nodes
ROAD	49,123	26,302	26,301	291,197
nuScenes	307	39	38	6,677

nuScenes temporal node graphs. For nuScenes, we use 8 object categories:

$$\{\text{car, truck, bus, trailer, construction_vehicle, pedestrian, motorcycle, bicycle}\}. \quad (16)$$

Temporal windows use

$$\text{window size} = 3, \quad \text{window stride} = 1. \quad (17)$$

Exported graphs use 10-dimensional node features, with 307 train graphs, 39 val graphs, and 38 test graphs. In the reported balanced run, the evaluated labeled test-node count is 6,677.

4.4.2 Models: What They Do for Road Scene Understanding

We compare two models that share the same message-passing backbone and differ only in their output representation.

Vanilla GNN (softmax head). A message-passing backbone computes node embeddings z_v , followed by a linear classifier and softmax:

$$p_v(i) = \text{softmax}(Wz_v)_i. \quad (18)$$

This produces a point probability vector, and uncertainty is typically approximated by scalar confidence heuristics (e.g., maximum softmax probability) or predictive entropy. In closed-set settings this is effective; however, under strict leave-out-class shift, the softmax head still must commit probability mass to singleton classes, which can lead to overconfident errors on unfamiliar (OOD) nodes.

RS-GNN (belief head). RS-GNN keeps the same backbone but replaces the softmax head with a belief head over a focal-set budget \mathcal{F} . For each node v , the head outputs beliefs over focal sets (sigmoid activations), which are transformed into masses via Möbius inversion; a pignistic projection yields a point prediction used for accuracy and calibration metrics. The key difference is representational: RS-GNN can allocate mass to non-singleton focal sets, explicitly encoding *epistemic ambiguity* when the graph evidence is incomplete or conflicting. This is directly beneficial for road-scene understanding, where ambiguity is induced by occlusions, short tracks, rare actors, and novel motion-context patterns: instead of forcing a sharp singleton distribution, RS-GNN can represent partial support for multiple classes while increasing the epistemic uncertainty signal used for OOD detection.

4.4.3 Training and Leave-Out-Class Protocol

Both models share the same GATv2 backbone (hidden size 128); differences are only in the output head (softmax vs random sets).

Within-dataset leave-out-class OOD. For ROAD:

$$\mathcal{Y}_{\text{OOD}} = \{8, 9\}, \quad \mathcal{Y}_{\text{ID}} = \{0, \dots, 7\}. \quad (19)$$

For nuScenes:

$$\mathcal{Y}_{\text{OOD}} = \{6, 7\}, \quad \mathcal{Y}_{\text{ID}} = \{0, \dots, 5\}. \quad (20)$$

Training uses only labeled ID nodes; OOD-labeled nodes are excluded from supervision and used only for uncertainty-based evaluation.

Cross-dataset OOD. In the ROAD(ID)-nuScenes(OOD) experiment, all ROAD classes are treated as ID for training/evaluation on ROAD, and nuScenes test nodes are treated as OOD at evaluation time.

4.4.4 Backbone and Training Details

Backbone model. All experiments were executed within a dedicated Conda environment, which provided isolated dependency management for Python packages and ensured that all models were evaluated under identical software conditions present in the requirements. Experiments were executed via the command-line supporting all baselines and RS-GNN variants:

```
python main.py --dataset <dataset_name> --model <model_name> --count <seeds>
```

Because training is performed using NeighborLoader-based mini-batching, each forward pass only observes a subgraph of the full dataset. The random set formulation is particularly well-suited to this setting, as it does not require global normalization over the full graph or repeated sampling of model outputs. Each mini-batch produces a self-contained belief assignment over classes of subsets, which remains valid regardless of the sampled neighborhood size. This avoids coupling uncertainty estimation to full-graph computation.

Therefore, this ensures that uncertainty estimation grows with:

$$\mathcal{O}(2^K)$$

rather than requiring:

$$\mathcal{O}(K) \text{ repeated stochastic forward passes (as in ensembles).}$$

By constraining uncertainty to a compact set-based representation, the model ensures bounded computational complexity and compatibility with large-scale mini-batch training while still retaining expressive uncertainty estimates suitable for OOD detection.

All experiments in this section use a message-passing Graph Neural Network as the encoder, with GATv2 [Brody et al., 2021] as the default backbone in our pipeline. GATv2 is a graph attention network variant in which each node aggregates a weighted combination of its neighbors’ features, and the weights (attention coefficients) are learned as a function of the interacting node representations. Compared to non-attentive aggregation (e.g., GCN), attention allows the model to down-weight irrelevant or noisy neighbors and emphasize informative relations, which is particularly important in road scene graphs where a node’s neighborhood can contain mixed-quality cues (occlusions, spurious edges, short tracks, and rapidly changing context).

Concretely, our node encoder is a two-layer GATv2 message passing network with hidden size 128. The first attention layer uses 4 heads and maps input features to a multi-head hidden representation; the second layer collapses to a single head and returns a 128-dimensional embedding per node. After each layer, we apply a ReLU nonlinearity, and after the first layer we apply dropout with rate 0.2. Denoting node features at layer l by $H^{(l)}$, the encoder can be summarized as

$$H^{(1)} = \sigma\left(\text{GATv2}^{(1)}(X, \mathcal{E})\right), \quad H^{(2)} = \sigma\left(\text{GATv2}^{(2)}(H^{(1)}, \mathcal{E})\right), \quad (21)$$

where $\sigma(\cdot)$ is ReLU. The resulting node embedding is $z_v = H_v^{(2)} \in \mathbb{R}^{128}$.

Prediction heads (vanilla vs. RS-GNN). Both models share the same backbone encoder and differ only in the head.

In the *vanilla* model, logits are computed via a linear layer and converted to probabilities with softmax:

$$\ell_v = Wz_v, \quad p_v(i) = \text{softmax}(\ell_v)_i. \quad (22)$$

In *RS-GNN*, the head outputs focal-set beliefs via a two-layer MLP with sigmoid outputs over a focal-set budget \mathcal{F} :

$$\hat{\text{Bel}}_v(A_k) = \text{sigmoid}(g(z_v))_k, \quad A_k \in \mathcal{F}. \quad (23)$$

Masses over focal sets are recovered by a Möbius inversion matrix M (precomputed from \mathcal{F}):

$$\hat{m}_v = \hat{\text{Bel}}_v M, \quad (24)$$

and pignistic probabilities are computed by multiplying masses with the pignistic matrix P induced by \mathcal{F} :

$$\text{BetP}_v = \text{norm}(\hat{m}_v P), \quad (25)$$

where $\text{norm}(\cdot)$ denotes row-wise normalisation to ensure a proper probability vector. Final predictions use $\arg \max_i \text{BetP}_v(i)$, so RS-GNN differs from vanilla primarily in its uncertainty representation rather than in the decision rule.

Focal-set selection (how \mathcal{F} is constructed). To keep random-set outputs scalable, we do not enumerate all of $2^{\mathcal{Y}}$. Instead, \mathcal{F} contains: (i) all singleton sets over the full class space, and (ii) up to 64 additional non-singleton sets (max cardinality 3) selected from warm-up confusion statistics. This yields 74 focal sets for ROAD (10 singletons + 64 non-singletons) and 72 for nuScenes (8 singletons + 64 non-singletons). The focal-set budgets used for RS-GNN are given in Tab. 4.

Table 4: Focal-set budgets used for RS-GNN. ‘K non-singletons’ is the number of non-singleton focal sets added to singleton focal sets.

Dataset	#Classes (total)	K non-singletons	#Total focal sets (K + singletons)
ROAD	10 (ID=8, OOD=2)	64 (budgeted pairs/triples)	74
nuScenes	8 (ID=6, OOD=2)	64 (budgeted pairs/triples)	72

Training objective. Vanilla training minimises cross-entropy on labeled ID nodes. RS-GNN training minimises binary cross-entropy in belief space with mass-validity regularisation. For a labeled node with class y_v , the focal-set target is

$$\text{Bel}_v^{\text{target}}(A_k) = \mathbf{1}\{y_v \in A_k\}, \quad (26)$$

and the training loss is

$$\mathcal{L} = \text{BCE}\left(\text{Bel}^{\text{target}}, \hat{\text{Bel}}\right) + \alpha \mathbb{E}_v[\text{ReLU}(-\hat{m}_v)] + \beta \mathbb{E}_v\left[\text{ReLU}\left(\sum_{A_k \in \mathcal{F}} \hat{m}_v(A_k) - 1\right)\right]. \quad (27)$$

The first penalty discourages negative mass values; the second discourages total mass exceeding 1 (a relaxed normalisation constraint consistent with our implementation).

What counts as a labeled node (label masks). In ROAD temporal graphs, each frame includes an unlabeled scene node with label -1 . We evaluate and train only on nodes with valid labels using a label mask:

$$\mathcal{V}_{\text{lab}} = \{v \in \mathcal{V} : y_v \geq 0\}. \quad (28)$$

For strict leave-out-class OOD training, we additionally define the ID mask

$$\mathcal{V}_{\text{ID}} = \{v \in \mathcal{V}_{\text{lab}} : y_v \notin \mathcal{Y}_{\text{OOD}}\}, \quad (29)$$

and use \mathcal{V}_{ID} for training updates.

Training hyperparameters. For ROAD (temporal node graphs), the reported run uses GATv2 with hidden size 128, dropout 0.2, learning rate 10^{-3} , and regularisation weights $\alpha = \beta = 10^{-3}$. We train the vanilla model for 20 epochs and RS-GNN for 30 epochs, with 1 warm-up epoch to build the confusion matrix used for focal-set selection. The batch size is 16.

For nuScenes, the reported balanced run uses the same backbone (GATv2, hidden size 128, dropout 0.2) with learning rate 5×10^{-4} , $\alpha = \beta = 10^{-3}$, vanilla epochs 60, RS-GNN epochs 80, and warm-up epochs 3. Because nuScenes exhibits strong class imbalance in our strict leave-out split, we additionally use class-weighted losses and label smoothing with smoothing factor 0.02. The batch size is 16. Core experimental hyperparameters for the hold-out-class runs are listed in Tab. 5.

Table 5: Core hyperparameters used in the two hold-out-class runs.

Hyperparameter	ROAD	nuScenes
Backbone	GATv2 (2 layers)	GATv2 (2 layers)
Hidden dim	128	128
Attention heads	4 (first), 1 (second)	4 (first), 1 (second)
Dropout	0.2	0.2
Batch size	16	16
Learning Rate	1×10^{-3}	5×10^{-4}
Epochs	30	80
α, β	$10^{-3}, 10^{-3}$	$10^{-3}, 10^{-3}$

4.4.5 Evaluation Protocol

We evaluate both models on labeled test nodes. For vanilla, class probabilities are softmax outputs p_v . For RS-GNN, class probabilities are pignistic probabilities BetP_v .

Entropy-based scores.

$$H_v = - \sum_{i=0}^{C-1} p_v(i) \log(p_v(i) + \varepsilon), \quad s_v^{\text{MSP}} = 1 - \max_i p_v(i). \quad (30)$$

For binary OOD detection ($t_v = \mathbf{1}\{y_v \in \mathcal{Y}_{\text{OOD}}\}$), we report AUROC/AUPRC/FPR95 using H_v and s_v^{MSP} .

Credal-width score (RS-GNN). Let $\hat{y}_v = \arg \max_i \text{BetP}_v(i)$, and let $\hat{m}_v(A)$ be the predicted mass over the selected focal budget \mathcal{F} . For singleton class i :

$$\underline{P}_v(i) = \hat{m}_v(\{i\}), \quad \bar{P}_v(i) = \sum_{A: i \in A} \hat{m}_v(A). \quad (31)$$

We define predicted-class credal width:

$$W_v = \bar{P}_v(\hat{y}_v) - \underline{P}_v(\hat{y}_v). \quad (32)$$

We report AUROC/AUPRC/FPR95 for W_v , plus mean W_v on ID and OOD subsets.

Calibration and proper scoring rules. We report ECE (15 bins), multiclass NLL, and multiclass Brier score:

$$\text{ECE} = \sum_{b=1}^B \frac{|S_b|}{N} |\text{acc}(S_b) - \text{conf}(S_b)|, \quad B = 15, \quad (33)$$

$$\text{NLL} = -\frac{1}{N} \sum_{v=1}^N \log(p_v(y_v) + \varepsilon), \quad (34)$$

$$\text{Brier} = \frac{1}{N} \sum_{v=1}^N \sum_{i=0}^{C-1} (p_v(i) - \mathbf{1}\{y_v = i\})^2. \quad (35)$$

4.4.6 Results

We evaluate three aspects of performance: (i) in-distribution (ID) accuracy, (ii) calibration (ECE, NLL, Brier), and (iii) out-of-distribution (OOD) detection under strict leave-out-class and cross-dataset shift.

In-distribution performance. Tab. 6 reports ID metrics. On *ROAD held-out OOD*, both models achieve comparable accuracy (0.754 vs. 0.746), but RS-GNN improves calibration substantially (ECE 0.132 vs. 0.178; lower NLL and Brier), indicating better probabilistic reliability even without sacrificing accuracy. On *nuScenes*, the difference is more pronounced: RS-GNN improves accuracy from 0.418 to 0.593 and significantly reduces NLL (7.047 \rightarrow 2.079). This suggests that belief-based modeling stabilizes training under stronger class imbalance and shorter temporal windows. In the

cross-dataset *ROAD(ID)-nuScenes(OOD)* setting, RS-GNN slightly improves ID accuracy (0.770 vs. 0.751), though vanilla softmax achieves slightly better ECE and NLL on ROAD alone. This reflects the expected trade-off: random-set heads prioritize uncertainty separation over pure closed-set likelihood optimisation.

Table 6: In-distribution (ID) performance across ROAD and nuScenes settings. Metrics are reported on ID nodes only. For ROAD(ID)-NuScenes(OOD), ID metrics are computed on ROAD test nodes.

Setting	Dataset	Split	Model	Uncertainty	Acc (↑)	ECE (↓)	NLL (↓)	Brier (↓)
ROAD held-out OOD	ROAD	ID: {0, ..., 7} OOD: {8, 9}	Vanilla	Softmax entropy	0.754	0.178	1.849	0.431
			RS-GNN	Pignistic entropy	0.746	0.132	1.478	0.384
NuScenes held-out OOD	NuScenes	ID: {0, ..., 5} OOD: {6, 7}	Vanilla	Softmax entropy	0.418	0.452	7.047	0.905
			RS-GNN	Pignistic entropy	0.593	0.422	2.079	0.875
ROAD(ID) vs NuScenes(OOD)	ROAD	ID: all ROAD classes OOD: NuScenes	Vanilla	Softmax entropy	0.751	0.122	1.035	0.381
			RS-GNN	Pignistic entropy	0.770	0.157	1.837	0.398

OOD uncertainty separation. Tab. 7 shows entropy and credal-width behavior. **(i) ROAD held-out OOD.** Vanilla entropy separation is weak (AUROC 0.425). RS-GNN substantially improves entropy-based OOD detection (AUROC 0.662) and additionally provides a credal-width signal (AUROC 0.342), demonstrating that belief mass spreads meaningfully increase under unseen classes. **(ii) nuScenes held-out OOD.** Vanilla softmax entropy collapses near zero for both ID and OOD nodes, yielding near-random detection (AUROC 0.463). RS-GNN maintains non-trivial entropy levels and improves detection (entropy AUROC 0.500; credal-width AUROC 0.521). Although absolute performance remains moderate, uncertainty does not degenerate as in the softmax model. **(iii) Cross-dataset shift (ROAD-nuScenes).** This is the most severe scenario. Vanilla entropy completely collapses (AUROC ≈ 0.001), meaning the softmax model assigns high confidence to foreign-domain nodes. RS-GNN improves detection (entropy AUROC 0.053; credal-width AUROC 0.083), showing partial robustness, though cross-dataset generalisation remains fundamentally challenging.

Table 7: Out-of-distribution uncertainty and detection evaluation across ROAD and nuScenes settings. For Vanilla, uncertainty is softmax entropy; for RS-GNN, uncertainty is pignistic entropy with credal-width metrics where available.

Setting	Model	In-distribution (ID)		Out-of-distribution (OOD)		OOD Detection Metrics			
		Entropy (ID) (↓)	Credal (ID) (↓)	Entropy (OOD) (↑)	Credal (OOD) (↑)	AUROC (Entropy) (↑)	AUPRC (Entropy) (↑)	AUROC (Credal) (↑)	AUPRC (Credal) (↑)
ROAD held-out OOD ($\mathcal{V}_{OOD} = \{8, 9\}$)	Vanilla	0.180	–	0.226	–	0.425	0.208	–	–
	RS-GNN	0.158	0.094	0.354	0.017	0.662	0.327	0.342	0.186
nuScenes held-out OOD ($\mathcal{V}_{OOD} = \{6, 7\}$)	Vanilla	0.000124	–	0.000098	–	0.463	0.071	–	–
	RS-GNN	0.045	2.057	2.079	2.061	0.500	0.077	0.521	0.076
ROAD (ID) vs NuScenes (OOD)	Vanilla	0.329	–	2.48×10^{-10}	–	0.001	0.470	–	–
	RS-GNN	0.200	0.065	1.86×10^{-7}	0.121	0.053	0.500	0.083	0.500

Across settings, three consistent patterns emerge:

- Softmax heads maintain competitive ID accuracy but struggle to express epistemic uncertainty when encountering unseen classes.
- RS-GNN improves calibration and preserves uncertainty signals under class removal and moderate domain shift.
- Under extreme cross-dataset shift, both models degrade, but RS-GNN avoids the complete overconfidence collapse observed in softmax.

For road-scene understanding, this is crucial: softmax models tend to produce confident singleton predictions even when graph evidence is insufficient, whereas RS-GNN can distribute mass across focal sets, increasing entropy and credal width in ambiguous or novel scenarios.

In safety-critical pipelines, this translates to better downstream gating of tracking and planning modules, reducing the risk of overconfident errors on rare actors or unfamiliar motion-context patterns.

These results in 3 further show that the random-set model should not be judged solely by its single best run. While the best-performing configuration for each dataset is informative, the distribution of results across runs provides a more reliable picture of model stability. For example, on `Patents` and `reddit2`, the spread in AUROC values across experiments indicates that uncertainty quality can be highly sensitive to the chosen configuration. This suggests that the method has the capacity to produce



Figure 3: This figure presents the best-performing RS-GNN configuration for each dataset, providing a clear cross-dataset comparison of model performance.

strong OOD separation, but that such performance is not equally robust under all hyperparameter settings. In contrast, where a dataset exhibits a tighter clustering of results, the method can be interpreted as behaving more consistently, even if the absolute best score is not the highest among all benchmarks. This distinction is important: a method that performs well only under a narrow range of settings should be characterised differently from one whose performance is more stable across repeated trials.

An important feature of the present experiments is that focal-set construction differs across datasets. For datasets with a small number of ID classes, such as `patents`, `cora`, `squirrel`, `chameleon`, and `roman_empire`, the model uses the full power set of non-empty focal sets. In these cases, the random-set representation remains relatively direct, and uncertainty can be expressed across all class subsets. By contrast, for datasets with a larger number of classes, such as `reddit2` and others with more complex label spaces, the full power set becomes computationally impractical, and a budgeted focal-set construction is used instead. This difference is not merely an implementation detail; it has methodological implications. The results suggest that the quality of uncertainty estimates depends not only on the learned graph representation, but also on the expressiveness of the focal-set family through which mass is distributed. In other words, the uncertainty mechanism itself forms part of the model capacity.

The trade-off between ID classification performance and OOD detection quality also emerges clearly from the experiments as represented in 4. Across several datasets, including `patents`, `reddit2`, and `roman_empire`, the configurations yielding the highest OOD AUROC were not always those yielding the highest ID accuracy. This finding is significant because it shows that optimisation for predictive performance alone is insufficient in uncertainty-aware graph learning. A configuration that appears preferable under conventional classification criteria may not be the one that provides the most reliable uncertainty estimates. Accordingly, the results support the use of joint evaluation criteria when selecting random-set configurations. This is especially relevant in practical settings where uncertainty quality is not secondary, but central to the intended application. Bazhenov et al. [2022]

The dataset-level results also suggest that the usefulness of the random-set formulation depends on the characteristics of the task. On `patents` and `reddit2`, where the scale and complexity of the data make uncertainty estimation particularly relevant, the method provides a meaningful test of whether structured belief representations can improve OOD awareness. On `cora`, the smaller and more standard benchmark setting serves as a useful baseline, but it is less informative about the behavior of the method under more demanding conditions. Datasets such as `roman_empire`, `amazon_ratings`, and `coauthor` help bridge this gap by introducing additional diversity in graph topology, label structure, and task difficulty. Similarly, `squirrel` and `chameleon` are valuable because they are known to behave differently from more homophilous citation-style graphs, making them

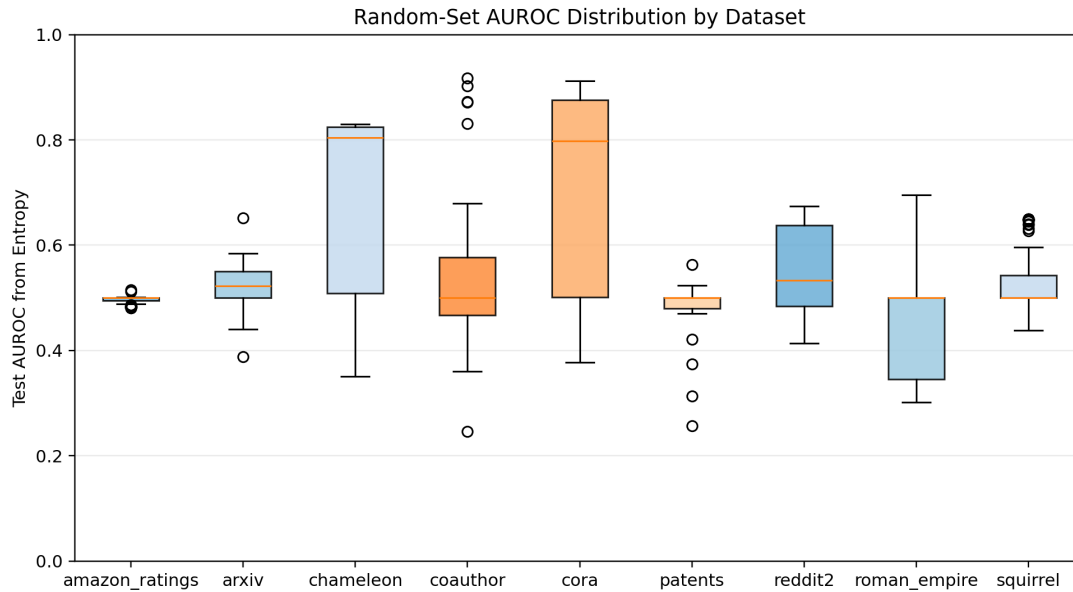


Figure 4: Distribution of RS-GNN AUROC scores across datasets, showing variability in uncertainty-aware performance over multiple runs. The figure highlights both the central tendency and spread of results, illustrating how RS-GNN behaves across diverse graph structures and task settings.

useful for testing whether the uncertainty framework remains informative under less conventional graph regimes. *Arxiv* further contributes by providing a large-scale citation setting distinct from *cora*, allowing comparison between smaller and larger citation-style benchmarks.

The evidence presented in 3 and 4 suggests that the random-set model is a credible approach to uncertainty-aware graph learning, particularly when the evaluation explicitly values both predictive performance and uncertainty quality. However, the results also indicate that its effectiveness depends materially on dataset properties, configuration choices, and focal-set construction strategy. For this reason, the method should not be interpreted as uniformly superior across all graph domains. Rather, its contribution lies in offering a structured representation of uncertainty whose strengths become apparent when evaluated across diverse datasets such as *patents*, *reddit2*, *cora*, *roman empire*, *squirrel*, *chameleon*, *arxiv*, *coauthor*, and *amazon ratings*. It's fair to conclude that the value of random sets lies not only in peak performance on a single benchmark, but in the broader insight they provide into how uncertainty can be represented, controlled, and evaluated in graph neural network settings.

5 Ablation studies

To further examine the behaviour of RS-GNN, an ablation study was conducted to assess the impact of focal set construction and loss formulation on both predictive performance and uncertainty estimation. Four configurations were considered: singletons-only with full training, standard focal sets with full training, standard focal sets with binary cross-entropy loss, and standard focal sets with BCE and margin regularisation. These configurations allow for a controlled comparison between simpler and more expressive focal set representations, as well as between different optimisation strategies. Ablation experiments were conducted on *cora* and *roman empire* rather than the full benchmark suite. This subset was selected to span the principal operating regimes of the random-set model: *cora* represents a smaller benchmark where full focal-set enumeration is feasible, while *roman empire* introduces a higher class-count setting in which budgeted focal-set construction is required. This selection allows the contribution of the main random-set design choices to be studied across representative conditions, while keeping the computational cost of the ablation study tractable.

The singletons-only configuration achieves the highest mean AUROC alongside relatively strong average accuracy. This suggests that even a restricted focal set can provide useful uncertainty

estimates. However, the corresponding distribution exhibits a higher degree of variability across runs, indicating that this configuration is less stable. In this setting, the model is limited to assigning belief to individual classes, which restricts its ability to explicitly represent ambiguity between classes.

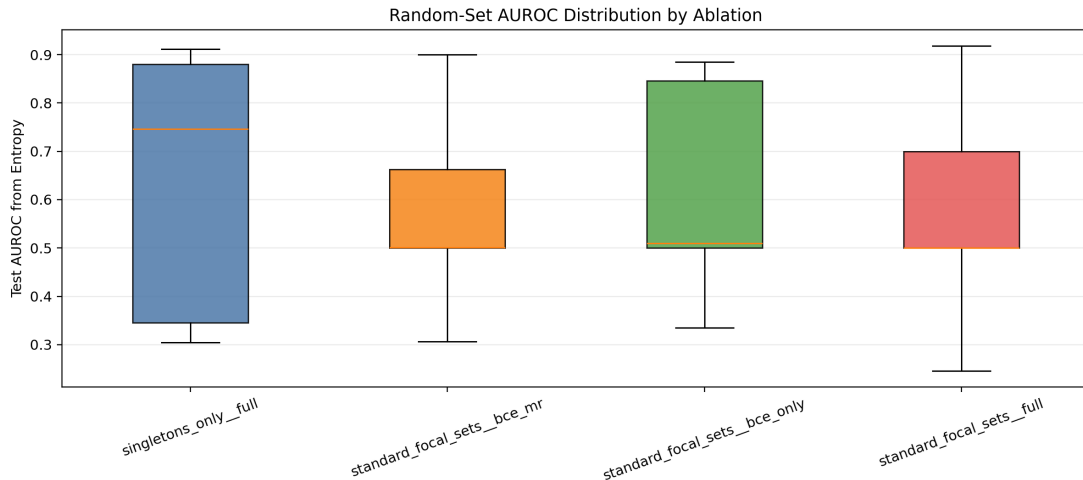


Figure 5: The results indicate that the choice of focal set has a measurable effect on both performance and stability.

By contrast, the standard focal set configuration as shown in 5 achieves the highest observed AUROC, while maintaining a more consistent distribution of results. Although its mean AUROC is slightly lower than that of the singletons-only configuration, the improved stability suggests that the additional expressiveness of the focal set enables more reliable modelling of uncertainty. In particular, the inclusion of multi-class subsets allows the model to capture partial knowledge in cases where evidence does not strongly support a single class.

The BCE-based variants (standard focal sets with BCE and BCE with margin regularisation) demonstrate lower performance overall, with mean AUROC values of 0.6070 and 0.5777, respectively. These results suggest that the choice of loss function has a significant influence on the quality of the learned belief assignments. In particular, optimisation using standard probabilistic loss functions appears less effective in this context, as such losses are not explicitly designed to operate over set-valued representations. In contrast, the full training objective, which directly operates in belief space, is better aligned with the underlying uncertainty framework.

These findings indicate that the effectiveness of RS-GNN depends on learned graph representations, and on the structure upon which uncertainty is expressed. Simpler focal set constructions may yield strong average performance, but more expressive configurations provide improved stability and stronger peak performance. This supports the broader observation that, within RS-GNN, uncertainty estimation is closely tied to the design of the focal set, and should therefore be treated as an integral component of the model rather than a secondary consideration.

Furthermore, the results in 6 highlight the role of focal-set construction in balancing expressiveness and computational efficiency. While configurations using the full focal-set space achieve the highest peak AUROC, the performance gap relative to reduced or singleton-based focal sets remains relatively small. This suggests that the primary gains of RS-GNN can be positively attributed to the combinatorial richness of the focal-set family and from the underlying belief-based representation itself. In practical terms, this indicates that lightweight focal-set configurations may provide a more favourable trade-off between computational cost and uncertainty quality, particularly for large-scale datasets where full enumeration is infeasible. In addition, the comparison between different training objectives reveals that variations such as binary cross-entropy alone and its margin-regularised counterpart produce only marginal differences in performance. This observation reinforces the idea that the effectiveness of RS-GNN is driven more by its representational framework than by specific optimisation choices. While regularisation contributes to stabilising training and ensuring valid mass assignments, it does not fundamentally alter the model’s ability to capture uncertainty.

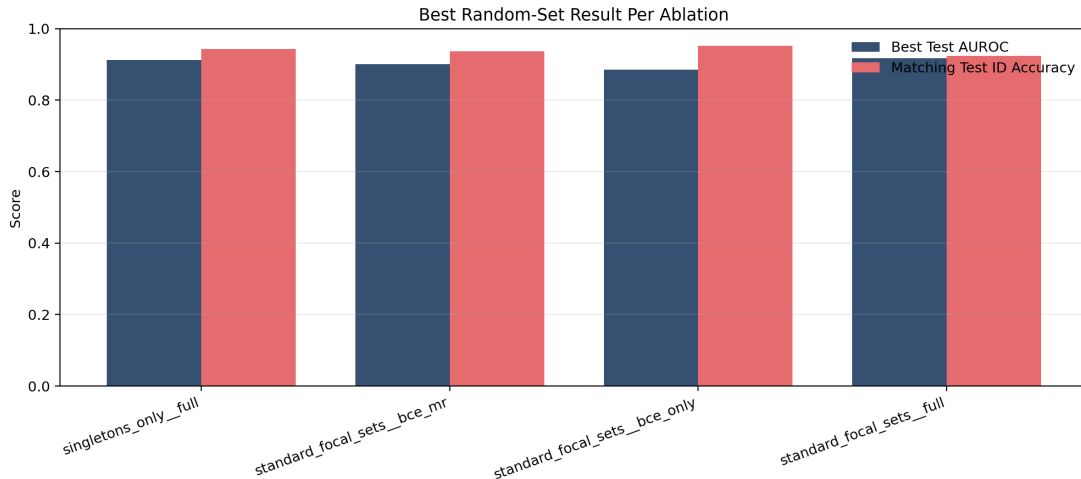


Figure 6: These results allow us to distinguish between AUROC and ID accuracy for the ablation studies performed.

Another notable pattern is the divergence between classification accuracy and AUROC across configurations. Although test accuracy remains consistently high, AUROC exhibits greater variability, indicating that improvements in predictive performance do not necessarily translate to better uncertainty estimation. This reinforces the need to evaluate uncertainty-aware models using metrics that explicitly capture their ability to distinguish between in-distribution and out-of-distribution samples.

Finally, the distribution of results across runs suggests differences in stability between configurations. While several setups achieve comparable peak performance, their mean AUROC values differ more noticeably, indicating that some configurations are more sensitive to initialisation and training dynamics. This highlights the importance of considering not only best-case results but also consistency when evaluating uncertainty-aware models.

In conclusion, this ablation study has demonstrated that the effectiveness of RS-GNN is primarily attributable to its belief-function representation, with focal-set design and training objective playing secondary but still meaningful roles. These findings support the broader idea that structured uncertainty representations can provide robust performance across different configurations, while also allowing flexibility in adapting the model to varying computational and dataset constraints.

6 Conclusions

In this paper, we proposed an original new framework in which node-level epistemic uncertainty is modelled in a belief function formalism. The resulting Random-Set Graph Neural Networks employ a belief-function head to predict a finite random set over the list of classes, from which both a precise probability prediction (via the pignistic transform) and a measure of epistemic uncertainty (expressed by the size of the predicted probability intervals for each class) can be obtained. Extensive experiments on 9 different graph learning datasets, including challenging real-world autonomous driving benchmarks as such Nuscene and ROAD, demonstrate RS-GNN’s superior uncertainty quantification capabilities.

The natural next step is the full integration of belief function representations in the message passing core of the GNN, building on existing body of knowledge on belief function propagation.

References

- Shireen Kudukkil Manchingal and Fabio Cuzzolin. Epistemic deep learning. *arXiv preprint arXiv:2206.07609*, 2022.
- Shireen Kudukkil Manchingal. Epistemic deep learning: Enabling machine learning models to know when they do not know. *arXiv preprint arXiv:2510.22261*, 2025.

- Alex Kendall and Yarin Gal. What uncertainties do we need in bayesian deep learning for computer vision? *Advances in neural information processing systems*, 30, 2017.
- Eyke Hüllermeier and Willem Waegeman. Aleatoric and epistemic uncertainty in machine learning: An introduction to concepts and methods. *Machine learning*, 110(3):457–506, 2021.
- Franco Scarselli, Marco Gori, Ah Chung Tsoi, Markus Hagenbuchner, and Gabriele Monfardini. The graph neural network model. *IEEE transactions on neural networks*, 20(1):61–80, 2008.
- Arijit Khan, Yuan Ye, and Lei Chen. *On uncertain graphs*. Morgan & Claypool Publishers, 2018.
- Fangxin Wang, Yuqing Liu, Kay Liu, Yibo Wang, Sourav Medya, and Philip S Yu. Uncertainty in graph neural networks: A survey. *arXiv preprint arXiv:2403.07185*, 2024a.
- Elena Ceci and Sergio Barbarossa. Graph signal processing in the presence of topology uncertainties. *IEEE Transactions on signal processing*, 68:1558–1573, 2020.
- Justin P Coon. Topological uncertainty in wireless networks. In *2016 IEEE Global Communications Conference (GLOBECOM)*, pages 1–6. IEEE, 2016.
- Tansel Yucelen, J Daniel Peterson, and Kevin L Moore. Control of networked multiagent systems with uncertain graph topologies. In *Dynamic Systems and Control Conference*, volume 57267, page V003T37A003. American Society of Mechanical Engineers, 2015.
- Jingkang Yang, Kaiyang Zhou, Yixuan Li, and Ziwei Liu. Generalized out-of-distribution detection: A survey. *International Journal of Computer Vision*, 132(12):5635–5662, 2024.
- Jakob Gawlikowski, Cedrique Rovile Njieutcheu Tassi, Mohsin Ali, Jongseok Lee, Matthias Humt, Jianxiang Feng, Anna Kruspe, Rudolph Triebel, Peter Jung, Ribana Roscher, et al. A survey of uncertainty in deep neural networks. *Artificial Intelligence Review*, 56(Suppl 1):1513–1589, 2023.
- Matias Valdenegro-Toro and Daniel Saromo Mori. A deeper look into aleatoric and epistemic uncertainty disentanglement. In *2022 IEEE/CVF Conference on Computer Vision and Pattern Recognition Workshops (CVPRW)*, pages 1508–1516. IEEE, 2022.
- Andrey Malinin and Mark Gales. Predictive uncertainty estimation via prior networks. *Advances in neural information processing systems*, 31, 2018.
- Arman Hasanzadeh, Ehsan Hajiramezani, Shahin Boluki, Mingyuan Zhou, Nick Duffield, Krishna Narayanan, and Xiaoning Qian. Bayesian graph neural networks with adaptive connection sampling. In *International conference on machine learning*, pages 4094–4104. PMLR, 2020.
- Sai Munikoti, Deepesh Agarwal, Laya Das, and Balasubramaniam Natarajan. A general framework for quantifying aleatoric and epistemic uncertainty in graph neural networks. *Neurocomputing*, 521:1–10, 2023.
- Ethan Goan and Clinton Fookes. Bayesian neural networks: An introduction and survey. In *Case Studies in Applied Bayesian Data Science: CIRM Jean-Morlet Chair, Fall 2018*, pages 45–87. Springer, 2020.
- Fangxin Wang, Yuqing Liu, Kay Liu, Yibo Wang, Sourav Medya, and Philip S Yu. Uncertainty in graph neural networks: A survey. *arXiv preprint arXiv:2403.07185*, 2024b.
- Balaji Lakshminarayanan, Alexander Pritzel, and Charles Blundell. Simple and scalable predictive uncertainty estimation using deep ensembles. *Advances in neural information processing systems*, 30, 2017.
- Tanwi Mallick, Prasanna Balaprakash, and Jane Macfarlane. Deep-ensemble-based uncertainty quantification in spatiotemporal graph neural networks for traffic forecasting. *arXiv preprint arXiv:2204.01618*, 2022.
- Matteo Tollosi and Davide Bacciu. Credal graph neural networks. *arXiv preprint arXiv:2512.02722*, 2025.

- Luis M De Campos, Juan F Huete, and Serafin Moral. Probability intervals: a tool for uncertain reasoning. *International Journal of Uncertainty, Fuzziness and Knowledge-Based Systems*, 2(02): 167–196, 1994.
- Judea Pearl. On probability intervals. *International Journal of Approximate Reasoning*, 2(3):211–216, 1988.
- F Cuzzolin. On the properties of the intersection probability. *submitted to the Annals of Mathematics and AI*, 2007a.
- Fabio Cuzzolin. Credal semantics of bayesian transformations in terms of probability intervals. *IEEE Transactions on Systems, Man, and Cybernetics, Part B (Cybernetics)*, 40(2):421–432, 2009.
- Fabio Cuzzolin. The intersection probability: betting with probability intervals. *arXiv preprint arXiv:2201.01729*, 2022.
- Michele Caprio, Maryam Sultana, Eleni Elia, and Fabio Cuzzolin. Credal learning theory. *Advances in Neural Information Processing Systems*, 37:38665–38694, 2024.
- Kaizheng Wang, Fabio Cuzzolin, Keivan Shariatmadar, David Moens, Hans Hallez, et al. Credal deep ensembles for uncertainty quantification. *Advances in Neural Information Processing Systems*, 37: 79540–79572, 2024c.
- Kaizheng Wang, Fabio Cuzzolin, Keivan Shariatmadar, David Moens, and Hans Hallez. A review of uncertainty representation and quantification in neural networks. *IEEE Transactions on Pattern Analysis and Machine Intelligence*, 2025a.
- Shireen Kudukkil Manchingal, Muhammad Mubashar, Kaizheng Wang, Keivan Shariatmadar, and Fabio Cuzzolin. Random-set convolutional neural network (rs-cnn) for epistemic deep learning. *arXiv preprint arXiv:2307.05772*, 2023.
- Shireen Kudukkil Manchingal, Muhammad Mubashar, Kaizheng Wang, Keivan Shariatmadar, and Fabio Cuzzolin. Random-set neural networks. In *The Thirteenth International Conference on Learning Representations*, 2025a. URL <https://openreview.net/forum?id=pdjkikvCch>.
- Shireen Kudukkil Manchingal, Armand Amaritei, Mihir Gohad, Maryam Sultana, Julian FP Kooij, Fabio Cuzzolin, and Andrew Bradley. Uncertainty-aware autonomous vehicles: Predicting the road ahead. *arXiv preprint arXiv:2510.22680*, 2025b.
- Shireen Kudukkil Manchingal, Muhammad Mubashar, Kaizheng Wang, and Fabio Cuzzolin. A unified evaluation framework for epistemic predictions, 2025c. URL <https://arxiv.org/abs/2501.16912>.
- Michele Caprio, Souradeep Dutta, Kuk Jin Jang, Vivian Lin, Radoslav Ivanov, Oleg Sokolsky, and Insup Lee. Imprecise Bayesian neural networks. *arXiv preprint arXiv:2302.09656*, 2023.
- Yusuf Sale, Michele Caprio, and Eyke Höllermeier. Is the volume of a credal set a good measure for epistemic uncertainty? In *Uncertainty in Artificial Intelligence*, pages 1795–1804. PMLR, 2023.
- Michele Caprio, Shireen K Manchingal, and Fabio Cuzzolin. Credal and interval deep evidential classifications. *arXiv preprint arXiv:2512.05526*, 2025.
- Kaizheng Wang, Keivan Shariatmadar, Shireen Kudukkil Manchingal, Fabio Cuzzolin, David Moens, and Hans Hallez. Creinns: Credal-set interval neural networks for uncertainty estimation in classification tasks. *Neural Networks*, 185:107198, 2025b.
- Kaizheng Wang, Fabio Cuzzolin, Keivan Shariatmadar, David Moens, and Hans Hallez. Credal wrapper of model averaging for uncertainty estimation on out-of-distribution detection. *arXiv preprint arXiv:2405.15047*, 2024d.
- Kaizheng Wang, Fabio Cuzzolin, Shireen Kudukkil Manchingal, Keivan Shariatmadar, David Moens, and Hans Hallez. Credal deep ensembles for uncertainty quantification. In *The Thirty-eighth Annual Conference on Neural Information Processing Systems*, 2024e.
- Fabio Cuzzolin. Uncertainty measures: The big picture. *arXiv preprint arXiv:2104.06839*, 2021.

- Fabio Cuzzolin. Uncertainty measures: A critical survey. *Information Fusion*, page 102609, 2024.
- Fabio Cuzzolin and Maryam Sultana. *Epistemic Uncertainty in Artificial Intelligence*. Springer, 2024.
- Hung Nguyen and Tonghui Wang. *Belief Functions and Random Sets*, pages 243–255. Springer, 01 1997. ISBN 978-1-4612-7350-9. doi: 10.1007/978-1-4612-1942-2_11.
- David Ross. Random sets without separability. *Annals of Probability*, 14(3):1064–1069, July 1986.
- Philippe Smets. The transferable belief model and random sets. *International Journal of Intelligent Systems*, 7(1):37–46, 1992.
- Shireen Kudukkil Manchingal, Muhammad Mubashar, Maryam Sultana, Salman Khan, and Fabio Cuzzolin. Epistemic artificial intelligence: Using random sets to quantify uncertainty in machine learning. Manuscript, 2024.
- Fabio Cuzzolin. Reasoning with random sets: An agenda for the future. *arXiv preprint arXiv:2401.09435*, 2023.
- John Goutsias, Ronald P. S. Mahler, and Hung T. Nguyen. *Random sets: theory and applications*, volume 97 of *IMA Volumes in Mathematics and Its Applications*. Springer-Verlag, December 1997.
- Minghu Ha, Witold Pedrycz, Jiqiang Chen, and Lifang Zheng. Some theoretical results of learning theory based on random sets in set-valued probability space. *Kybernetes*, 38(3-4):635–657, 2009.
- Ilya Molchanov. Statistical problems for random sets. In *Random Sets*, pages 27–45. Springer, 1997.
- Ilya Molchanov. On strong laws of large numbers for random upper semicontinuous functions. *Journal of mathematical analysis and applications*, 235(1):349–355, 1999.
- Ilya S Molchanov. *Theory of random sets*, volume 19. Springer, 2005.
- Glenn Shafer. A theory of statistical evidence. In W. L. Harper and C. A. Hooker, editors, *Foundations of Probability Theory, Statistical Inference, and Statistical Theories of Science*, volume 2, pages 365–436. Reidel, Dordrecht, 1976.
- Fabio Cuzzolin. *Belief functions: theory and applications*. Springer, 2014.
- Fabio Cuzzolin. *Visions of a generalized probability theory*. Lambert Academic Publishing, September 2014.
- Fabio Cuzzolin. Belief likelihood function for generalised logistic regression. *arXiv preprint arXiv:1808.02560*, 2018a.
- Fabio Cuzzolin. *The Geometry of Uncertainty: The Geometry of Imprecise Probabilities*. Artificial Intelligence: Foundations, Theory, and Algorithms. Springer International Publishing, 2020. ISBN 9783030631536. URL <https://books.google.co.uk/books?id=jNQPEAAAQBAJ>.
- Isaac Levi. *The enterprise of knowledge: An essay on knowledge, credal probability, and chance*. The MIT Press, Cambridge, Massachusetts, 1980.
- Fabio Cuzzolin. Visions of a generalized probability theory. *arXiv preprint arXiv:1810.10341*, 2018b.
- Philippe Smets and Robert Kennes. The transferable belief model. *Artificial intelligence*, 66(2): 191–234, 1994.
- Muhammad Mubashar, Shireen Kudukkil Manchingal, and Fabio Cuzzolin. Random-set large language models. *arXiv preprint arXiv:2504.18085*, 2025.
- Muhammad Mubashar and Fabio Cuzzolin. Epistemic generative adversarial networks. *arXiv preprint arXiv:2603.18348*, 2026.
- Maryam Sultana, Neil Yorke-Smith, Kaizheng Wang, Shireen Kudukkil Manchingal, Muhammad Mubashar, and Fabio Cuzzolin. Epistemic wrapping for uncertainty quantification. *arXiv preprint arXiv:2505.02277*, 2025.

- Dominik Fuchsgruber, Tom Wollschläger, Johannes Bordne, and Stephan Günnemann. Uncertainty estimation for heterophilic graphs through the lens of information theory. *arXiv preprint arXiv:2505.22152*, 2025.
- Jiong Zhu, Yujun Yan, Lingxiao Zhao, Mark Heimann, Leman Akoglu, and Danai Koutra. Beyond homophily in graph neural networks: Current limitations and effective designs. *Advances in neural information processing systems*, 33:7793–7804, 2020.
- Derek Lim, Felix Hohne, Xiuyu Li, Sijia Linda Huang, Vaishnavi Gupta, Omkar Bhalerao, and Ser Nam Lim. Large scale learning on non-homophilous graphs: New benchmarks and strong simple methods. *Advances in neural information processing systems*, 34:20887–20902, 2021.
- Prakash P Shenoy and Glenn Shafer. Axioms for probability and belief-function propagation. In *Machine intelligence and pattern recognition*, volume 9, pages 169–198. Elsevier, 1990.
- Prakash P Shenoy and Glenn Shafer. Propagating belief functions with local computations. *IEEE Expert*, 1(3):43–52, 1986.
- Prakash P Shenoy. Graphical belief function models: Theory, computation, and applications. *Graphical Models*, 1(77), 2023.
- Holger Caesar, Varun Bankiti, Alex H Lang, Sourabh Vora, Venice Erin Liong, Qiang Xu, Anush Krishnan, Yu Pan, Giancarlo Baldan, and Oscar Beijbom. nuscenes: A multimodal dataset for autonomous driving. In *Proceedings of the IEEE/CVF conference on computer vision and pattern recognition*, pages 11621–11631, 2020.
- Gurkirt Singh, Stephen Akrigg, Manuele Di Maio, Valentina Fontana, Reza Javanmard Alitappeh, Salman Khan, Suman Saha, Kossar Jeddisaravi, Farzad Yousefi, Fabio Cuzzolin Culley, Jacob, et al. ROAD: The road event awareness dataset for autonomous driving. *IEEE Transactions on Pattern Analysis and Machine Intelligence*, 45(1):1036–1054, 2022.
- Davide Bacciu, Federico Errica, Alessio Micheli, and Marco Podda. A gentle introduction to deep learning for graphs. *Neural Networks*, 129:203–221, 2020.
- Chao Chen, Chenghua Guo, Rui Xu, Xiangwen Liao, Xi Zhang, Sihong Xie, Hui Xiong, and Philip Yu. Uncertainty quantification on graph learning: A survey. *arXiv preprint arXiv:2404.14642*, 2024.
- Chuan Guo, Geoff Pleiss, Yu Sun, and Kilian Q Weinberger. On calibration of modern neural networks. In *International conference on machine learning*, pages 1321–1330. PMLR, 2017.
- Xujiang Zhao, Feng Chen, Shu Hu, and Jin-Hee Cho. Uncertainty aware semi-supervised learning on graph data. In *Advances in Neural Information Processing Systems*, volume 33. Curran Associates, Inc., 2020. URL <https://proceedings.neurips.cc/paper/2020/hash/968c9b4f09cbb7d7925f38aea3484111-Abstract.html>.
- Maximilian Stadler, Bertrand Charpentier, Simon Geisler, Daniel Zügner, and Stephan Günnemann. Graph posterior network: Bayesian predictive uncertainty for node classification. In *Advances in Neural Information Processing Systems*, volume 34, pages 18033–18048. Curran Associates, Inc., 2021a. URL https://proceedings.neurips.cc/paper_files/paper/2021/hash/95b431e51fc53692913da5263c214162-Abstract.html.
- Qitian Wu, Yiting Chen, Chenxiao Yang, and Junchi Yan. Energy-based out-of-distribution detection for graph neural networks. *arXiv preprint arXiv:2302.02914*, 2023.
- Xiao Wang, Hongrui Liu, Chuan Shi, and Cheng Yang. Be confident! towards trustworthy graph neural networks via confidence calibration. *Advances in Neural Information Processing Systems*, 34:23768–23779, 2021.
- Dominik Fuchsgruber, Tom Wollschläger, and Stephan Günnemann. Energy-based epistemic uncertainty for graph neural networks. *Advances in Neural Information Processing Systems*, 37: 34378–34428, 2024.

- Yarin Gal and Zoubin Ghahramani. Dropout as a bayesian approximation: Representing model uncertainty in deep learning. In *international conference on machine learning*, pages 1050–1059. PMLR, 2016.
- Matthew D Hoffman, David M Blei, Chong Wang, and John Paisley. Stochastic variational inference. *the Journal of machine Learning research*, 14(1):1303–1347, 2013.
- Maximilian Stadler, Bertrand Charpentier, Simon Geisler, Daniel Zügner, and Stephan Günnemann. Graph posterior network: Bayesian predictive uncertainty for node classification. *Advances in Neural Information Processing Systems*, 34:18033–18048, 2021b.
- Xiaotao Jia, Jianlei Yang, Runze Liu, Xueyan Wang, Sorin Dan Cotofana, and Weisheng Zhao. Efficient computation reduction in bayesian neural networks through feature decomposition and memorization. *IEEE transactions on neural networks and learning systems*, 32(4):1703–1712, 2020.
- Jonas Busk, Mikkel N Schmidt, Ole Winther, Tejs Vegge, and Peter Bjørn Jørgensen. Graph neural network interatomic potential ensembles with calibrated aleatoric and epistemic uncertainty on energy and forces. *Physical Chemistry Chemical Physics*, 25(37):25828–25837, 2023.
- Michel Grabisch. The Möbius transform on symmetric ordered structures and its application to capacities on finite sets. *Discrete Mathematics*, 287(1–3):17–34, 2004.
- Fabio Cuzzolin. Alternative formulations of the theory of evidence based on basic plausibility and commonality assignments. In *Proceedings of the Pacific Rim International Conference on Artificial Intelligence (PRICAI'08)*, pages 91–102, 2008a.
- Fabio Cuzzolin. Three alternative combinatorial formulations of the theory of evidence. *Intelligent Data Analysis*, 14(4):439–464, 2010a.
- Philippe Smets. Decision making in a context where uncertainty is represented by belief functions. In *Belief functions in business decisions*, pages 17–61. Springer, 2002.
- Philippe Smets. Decision making in the TBM: the necessity of the pignistic transformation. *International Journal of Approximate Reasoning*, 38(2):133–147, 2005.
- Fabio Cuzzolin. On the credal structure of consistent probabilities. In *European Workshop on Logics in Artificial Intelligence*, pages 126–139. Springer, 2008b.
- Fabio Cuzzolin. Credal semantics of Bayesian transformations in terms of probability intervals. *IEEE Transactions on Systems, Man, and Cybernetics, Part B: Cybernetics*, 40(2):421–432, 2010b.
- Philippe Smets et al. Constructing the pignistic probability function in a context of uncertainty. In *UAI*, volume 89, pages 29–40, 1989.
- John J Sudano. Pignistic probability transforms for mixes of low-and high-probability events. *arXiv preprint arXiv:1505.07751*, 2015.
- Fabio Cuzzolin. On the orthogonal projection of a belief function. In *European Conference on Symbolic and Quantitative Approaches to Reasoning and Uncertainty*, pages 356–367. Springer, 2007b.
- Fabio Cuzzolin. Two new bayesian approximations of belief functions based on convex geometry. *IEEE Transactions on Systems, Man, and Cybernetics, Part B (Cybernetics)*, 37(4):993–1008, 2007c.
- Fabio Cuzzolin. Dual properties of the relative belief of singletons. In *Pacific Rim International Conference on Artificial Intelligence*, pages 78–90. Springer, 2008c.
- Fabio Cuzzolin. On the relative belief transform. *International Journal of Approximate Reasoning*, 53(5):786–804, 2012.
- Barry R Cobb and Prakash P Shenoy. On the plausibility transformation method for translating belief function models to probability models. *International journal of approximate reasoning*, 41(3): 314–330, 2006.

- Fabio Cuzzolin. Geometry of relative plausibility and relative belief of singletons. *Annals of Mathematics and Artificial Intelligence*, 59(1):47–79, 2010c.
- Oleksandr Shchur, Maximilian Mumme, Aleksandar Bojchevski, and Stephan Günnemann. Pitfalls of graph neural network evaluation. *arXiv preprint arXiv:1811.05868*, 2018.
- Oleg Platonov, Denis Kuznedelev, Michael Diskin, Artem Babenko, and Liudmila Prokhorenkova. A critical look at the evaluation of gnns under heterophily: Are we really making progress? *arXiv preprint arXiv:2302.11640*, 2023.
- Benedek Rozemberczki, Carl Allen, and Rik Sarkar. Multi-scale attributed node embedding. *Journal of Complex Networks*, 9(2):cnab014, 2021.
- Will Hamilton, Zhitao Ying, and Jure Leskovec. Inductive representation learning on large graphs. *Advances in neural information processing systems*, 30, 2017.
- Weihua Hu, Matthias Fey, Marinka Zitnik, Yuxiao Dong, Hongyu Ren, Bowen Liu, Michele Catasta, and Jure Leskovec. Open graph benchmark: Datasets for machine learning on graphs. *Advances in neural information processing systems*, 33:22118–22133, 2020.
- Longfei Ma, Yiyu Sun, Kaize Ding, Zemin Liu, and Fei Wu. Revisiting score propagation in graph out-of-distribution detection. *Advances in Neural Information Processing Systems*, 37:4341–4373, 2024.
- Zhilin Yang, William Cohen, and Ruslan Salakhudinov. Revisiting semi-supervised learning with graph embeddings. In *International conference on machine learning*, pages 40–48. PMLR, 2016.
- Jure Leskovec, Jon Kleinberg, and Christos Faloutsos. Graphs over time: densification laws, shrinking diameters and possible explanations. In *Proceedings of the eleventh ACM SIGKDD international conference on Knowledge discovery in data mining*, pages 177–187, 2005.
- Weitang Liu, Xiaoyun Wang, John Owens, and Yixuan Li. Energy-based out-of-distribution detection. *Advances in neural information processing systems*, 33:21464–21475, 2020.
- Shiyu Liang, Yixuan Li, and Rayadurgam Srikant. Enhancing the reliability of out-of-distribution image detection in neural networks. *arXiv preprint arXiv:1706.02690*, 2017.
- Kimin Lee, Kibok Lee, Honglak Lee, and Jinwoo Shin. A simple unified framework for detecting out-of-distribution samples and adversarial attacks. *Advances in neural information processing systems*, 31, 2018.
- Yiyu Sun, Yifei Ming, Xiaojin Zhu, and Yixuan Li. Out-of-distribution detection with deep nearest neighbors. In *International conference on machine learning*, pages 20827–20840. PMLR, 2022.
- Yaniv Ovadia, Emily Fertig, Jie Ren, Zachary Nado, David Sculley, Sebastian Nowozin, Joshua Dillon, Balaji Lakshminarayanan, and Jasper Snoek. Can you trust your model’s uncertainty? evaluating predictive uncertainty under dataset shift. *Advances in neural information processing systems*, 32, 2019.
- Fredrik K Gustafsson, Martin Danelljan, and Thomas B Schon. Evaluating scalable bayesian deep learning methods for robust computer vision. In *Proceedings of the IEEE/CVF conference on computer vision and pattern recognition workshops*, pages 318–319, 2020.
- Taiga Abe, Estefany Kelly Buchanan, Geoff Pleiss, Richard Zemel, and John P Cunningham. Deep ensembles work, but are they necessary? *Advances in Neural Information Processing Systems*, 35: 33646–33660, 2022.
- Shaked Brody, Uri Alon, and Eran Yahav. How attentive are graph attention networks? *arXiv preprint arXiv:2105.14491*, 2021.
- Gleb Bazhenov, Sergei Ivanov, Maxim Panov, Alexey Zaytsev, and Evgeny Burnaev. Towards OOD detection in graph classification from uncertainty estimation perspective, 2022. URL <http://arxiv.org/abs/2206.10691>.